

Asymmetrical 4x2 Array Microstrip Antenna Using Glass Fiber-Ramie-Alumina-Carbon Composite Substrate for 5G Mobile Communication

Irfan Mujahidin^a, Budi Basuki Subagio^a, Muhlasah Novitasari Mara^{a,*}, Helmy^a, Akio Kitagawa^b

^a Department of Telecommunication Engineering, Faculty of Electrical Engineering, Politeknik Negeri Semarang, Semarang, Indonesia

^b Department of Electrical Engineering and Computer Science, Graduate School of Natural Science and Technology, Kanzawa university, Japan

Corresponding author: *muhlasah@polines.ac.id

Abstract—This paper proposes an asymmetrical 4x2 array antenna for 5G centimeter-wave (cm-wave) communication systems. To optimize substrate efficiency, we employed a multi-element-antenna array combination using sixteen elements. Our substrate optimization involved a Glass Fiber-Ramie-Alumina Composite with a permittivity of 9.4. The proposed asymmetrical 4x4 array operates within the 3.5 GHz frequency band for 5G cm-wave applications. The individual antenna element achieves a gain of 5.23 dBi, which increases to 10.9 dBi when configured in an eight-element array. The optimized antenna substrate offers several advantages, including improved electrical, mechanical, and chemical properties. This results in a substantial reduction in leakage and attenuation, substantially simplified fabrication processes, and markedly reduced manufacturing costs, making it well-suited for 5G communications. The reduction in manufacturing costs is particularly significant, as it can contribute to overall affordability and widespread adoption of 5G technology. Additionally, the improved electrical and mechanical properties of the substrate ensure reliable and efficient performance in various environmental conditions. Furthermore, the proposed antenna design is compact and lightweight, making it suitable for various applications, including mobile devices, wearable technology, and Internet of Things (IoT) devices. The combination of these advantages positions the proposed antenna as a promising candidate for future 5G communication systems, particularly in scenarios where low-cost, high-performance, compact form factors, efficient power consumption, and robustness against interference are essential.

Keywords— Array microstrip antenna; composite substrate; 5G mobile; glass fiber-ramie-alumina.

Manuscript received 22 Jul. 2024; revised 18 Oct. 2024; accepted 24 Nov. 2024. Date of publication 30 Apr. 2025.
IJASEIT is licensed under a Creative Commons Attribution-Share Alike 4.0 International License.



I. INTRODUCTION

The challenges posed by emerging 5G technology demand antennas with features that can accommodate user terminals as both senders and receivers. Beamforming radiation patterns, for example, are essential for spatial scanning and improved efficiency. Meeting these requirements presents significant design challenges in achieving a reasonable balance between technological design issues and commercial criteria, including low cost, small size, radiation efficiency, antenna gain, broadband performance, and more, especially in the centimeter wave range [1].

It is well-known that higher frequencies lead to smaller antennas, and shorter wavelengths necessitate more antennas for a given coverage area [2], [3]. To realize 6G telecommunications, Principia Scientific International, a non-

profit organization, suggests that communication service operators build base transceiver stations (BTS) at intervals of 100 meters or less. This would require a substantial increase in BTS density [4]. In 2020, MIIT, or the Ministry of Industry and Information of China, declared that more than 690,000 5G base stations are operating in China. This number is still far from the target, considering that another 10 million 5G BTS are needed to cover the entire Chinese region [5], [6]. Similar demands for 5G antennas will likely arise in other countries worldwide.

Among potential solutions, a microstrip antenna with coplanar placement of radiation elements and a power supply network appears promising for 5G applications due to its balance of functionality and manufacturing complexity [7], [8]. However, current methods for increasing the performance and reducing the cost of coplanar antennas remain insufficient.

To reduce costs, currently, most countries use FR4 substrates as microstrip antenna materials. While FR4 offers advantages such as low price, low water absorption, and good insulation, it has limitations in terms of tensile strength and temperature tolerance (up to 130°C) [9], [10]. As the need for microstrip antennas in the extra-high-frequency range grows with the development of next-generation telecommunication systems, reducing dependence on FR4 becomes increasingly important [11], [12]. This paper explores the use of ramie fiber waste as an alternative material to FR4 for the mass manufacture of microstrip antennas. Ramie fiber waste is processed into a Glass Fiber-Ramie-Alumina Composite substrate, which offers advantages in electrical, mechanical, and chemical properties. Glass fiber, which serves as a skeleton, has heat-resistant properties and improves tensile strength and heat resistance to temperature changes [13]. Ramie has a high tensile strength [14]. While alumina and carbon have insulated properties and a relative dielectric coefficient value of 10, so if these materials are combined into one into a composite, it will increase the relative dielectric constant of the composite close to pure alumina, from the experiment using VNA the relative dielectric constant of 9.2 is obtained. FR4 has only a dielectric constant value of 4. This material is implemented in a 4x2 antenna array that is designed to address the challenges of microstrip antennas in 5G network communications. The fabricated substrate material is more flexible because the thickness can be changed according to our design to change the capacitance value in the composite with the formula:

$$C = \frac{\epsilon_0 \epsilon_r A}{d} \quad (1)$$

where:

C = Proficiency

ϵ_0 = Void Dielectric Constant = $8,854 \times 10^{-12}$ F/m

ϵ_r = Dielectric Constant Relative Material

A = Wide of cross-sectional area

d = Cross-sectional distance

When compared to substrates on the market, for example FR4 and duroid, besides being very expensive, the thickness cannot be changed so that it is difficult to set the parameters.

II. MATERIALS AND METHODS

A. Substrate Composition Design

The manufacturing process commences by sourcing Ramie fiber waste from local Ramie farmers in Wonosobo City. This Ramie fiber waste is then combined with a composite material consisting of Epoxy Resin ($C_{21}H_{24}O_4$), Epoxy Hardener ($C_6H_{18}N_4$), and Alumina powder (Al_2O_3) in a 1:1:1 ratio. The procedure involves sequential mixing steps: first, blend the Epoxy Resin and Epoxy Hardener until the color changes [15]. Following this, gradually introduce the Alumina powder and continue stirring until all the ingredients are thoroughly mixed [16]. Subsequently, glass fiber (SiO_2) and hemp fiber waste, with cellulose ($C_6H_{10}O_5$) as the primary compound, are coated with the pre-made composite material. This coating enhances the structural integrity and rigidity of the Ramie fiber waste when subjected to pressure on Fig. 1 [17].

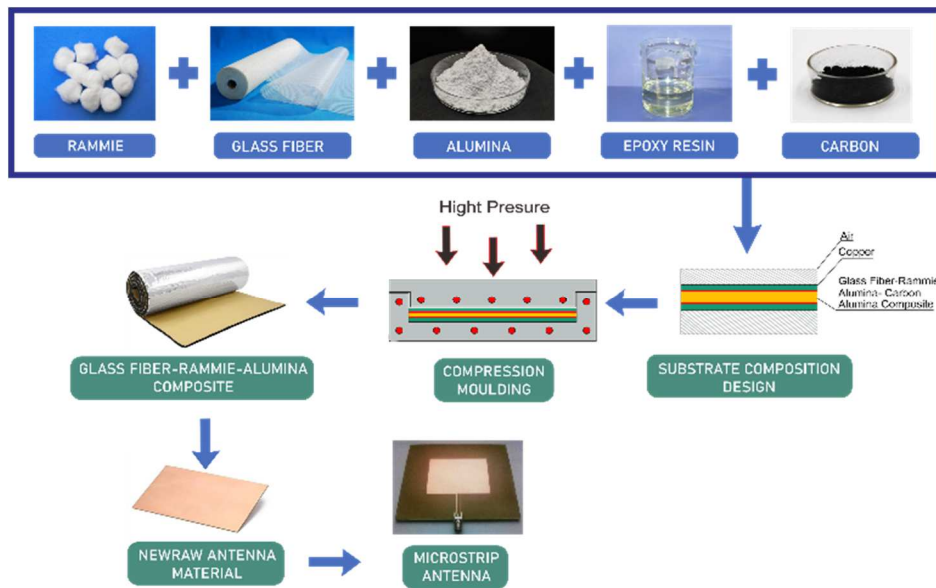


Fig. 1 Method for making glass fiber-ramie-alumina composite substrate

The substrate composition design is achieved by arranging the Ramie fiber coated with the composite material on both the upper and lower sides [18], [19]. On the lower side, it is initially protected with a layer of plastic, and after the basting process with the composite material, it is covered with plastic once more. This process serves the purpose of preventing the substrate material from adhering directly to the iron plate when

subjected to pressure, facilitating its removal from the mold on Fig. 1 [20], [21].

The subsequent step involves the compression molding of the Ramie fiber, which has been coated with the composite, using two metal plates, as illustrated in Fig. 2. This compression molding process typically spans at least one day.

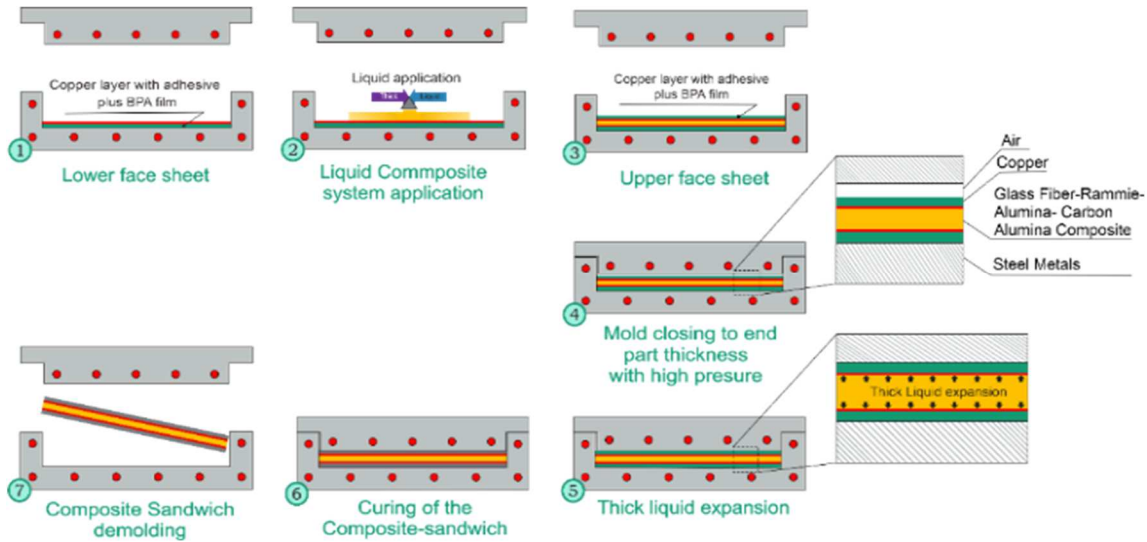


Fig. 2 High-pressure thick liquid composite coating process

The primary objective at this stage is to validate the suitability of the Ramie-Alumina Composite substrate as an alternative material for replacing FR-4 in the production of microstrip antennas [22], [23]. To achieve this, it is imperative to conduct a comprehensive analysis and measurement of the intrinsic dielectric properties of the Ramie-Alumina Composite substrate during the testing phase [24], [25].

B. Antenna Design

The microstrip patch antenna's geometry on the glass fiber-Ramie-alumina composite substrate is depicted in Fig. 3. The proposed antenna design encompasses various parameters and specifications. The simulation of the proposed 5G antenna design, utilizing a glass fiber-Ramie-alumina composite substrate, has been conducted. The key parameters assessed during the simulation include return loss, VSWR (Voltage Standing Wave Ratio), radiation pattern, and polarization pattern [26].

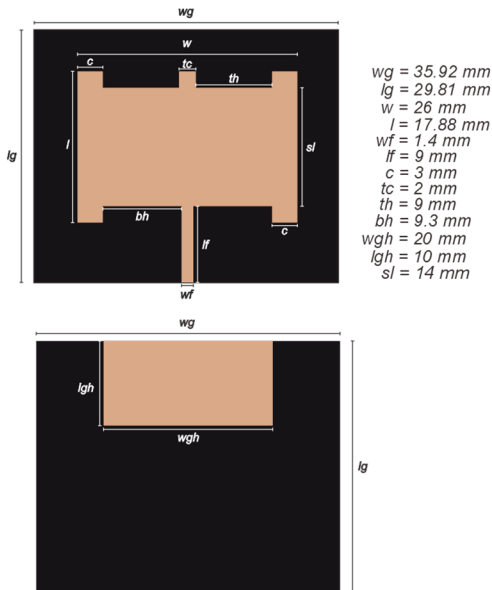


Fig. 3 The geometry of microstrip patch antenna on glass fiber-Ramie-alumina composite substrate

The simulated return loss results for the proposed 3.5 GHz 5G antenna design on a glass fiber-Ramie-alumina composite substrate are presented in Figure 4. Through multiple iterations carried out using CST Microwave Studio software, the desired performance target for the antenna was set to achieve a return loss of less than -10 dB [12], [27]. In the case of the asymmetrical 4x4 antenna operating at a frequency of 3.5841 GHz, it achieved a return loss value of -15.494938 dB. The parameter S1,1 is commonly referred to as the return loss in antenna performance analysis.

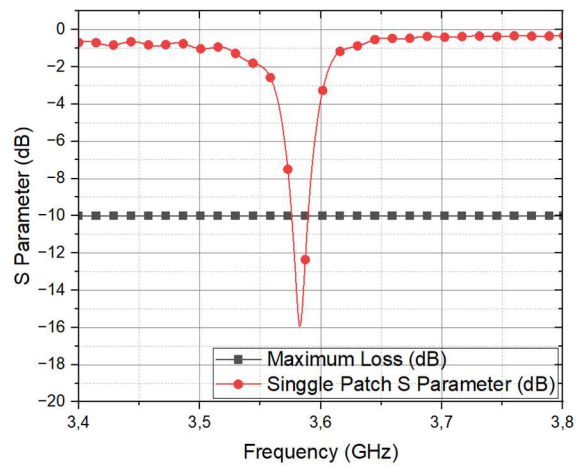


Fig. 4 The result of the S Parameter

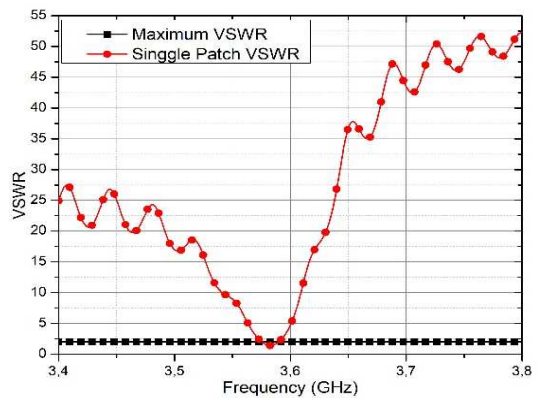


Fig. 5 The result of the VSWR simulation

The simulation results for VSWR are depicted in Fig. 5. The desired VSWR parameter was set to be less than two, and the simulation results show a value of 1.404584 at the frequency of 3.5841 GHz, as illustrated in Fig. 5.

This indicates that the antenna design on the glass fiber-Ramie-alumina composite substrate meets the VSWR performance requirement. Similarly, the radiation pattern shown in Fig. 6 also meets the performance requirements of antennas implanted in mobile communications with a directional radiation pattern that has a centered HPBW value close to a 0-degree angle.

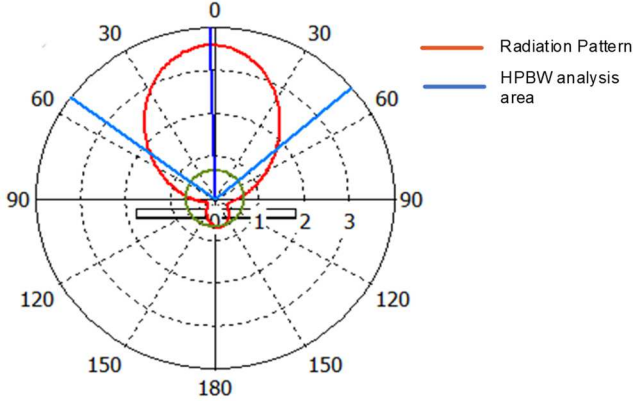


Fig. 6. The radiation pattern of the proposed antenna in Polar models

To improve the antenna performance, especially the power gain due to the antenna using glass fiber-Ramie-alumina composite substrate for 5G mobile Communication, it is further optimized using the array method with asymmetry aimed at providing wider and wider radiation pattern but increased gain value. The following in Fig. 7 is the result of the optimization process to increase the array antenna, which was originally from a single antenna and then optimized to become a 4x1 array antenna.

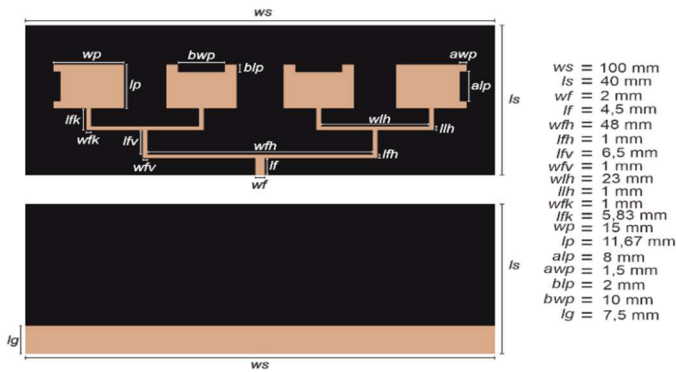


Fig. 7 4x1 Array Microstrip Antenna Design

The gain obtained after optimization is 5.23 dBi, then optimized again to obtain the most efficient value in terms of radiation pattern, gain, and other performance so that the most optimal dimensions are obtained in Figure 8 so that the gain is 10.9 dBi.

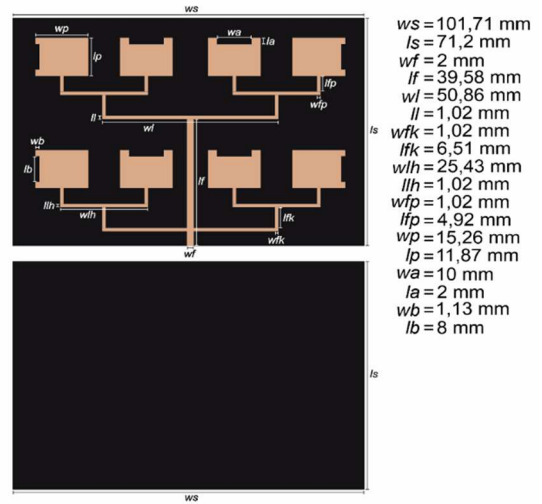


Fig. 8 4x2 Array Microstrip Antenna Design

III. RESULTS AND DISCUSSION

A. Glass Fiber-Ramie- Carbon- Alumina Composite Substrates

Relative permittivity or ϵ_r (Epsilon r) is a particularly important parameter in microstrip antenna design. It is the ratio between the dielectric permittivity of a material, such as a glass fiber-Ramie-alumina composite substrate, and the dielectric permittivity of a vacuum. The size of the conductor patch in a microstrip antenna is determined by the relative permittivity value. Evaluating the Alumina - Glass fiber substrate material using a Vector Network Analyzer [28]. The test used a frequency of 3500 MHz with substrate specifications of 3 mm thick, 101.5 cm long, and 110.5 cm wide and found a substrate area of 11215.75 cm^2 . Then, the test results of the relative permittivity of the glass fiber-Ramie-alumina composite substrate material can be obtained $Z = 0.69 - 0.43j$, based on Equation 2, the test data has a resistance value (R) of 0.69 Ω and a capacitive reactance value (XC) of $-0.43j$. Thus, the capacitance value can be obtained with equation 2.

$$\int X_C df = \int \frac{1}{2\pi C f} df \quad (2)$$

Then to calculate the total capacitive reactance in a substrate volume where the value of C is unstable, we can use equation 3. With the initial condition that C is a function of the position of the capacitance in three-dimensional space, $C(x, y, z)$, and we want to integrate the capacitive reactance X_C in a substrate volume V . Then the equation for the value of X_C on the substrate volume V can be described in equation 3:

$$\iiint X_C dV = \iiint \frac{1}{\omega C(x,y,z)} dV \quad (3)$$

Where dV is the infinitesimal substrate volume element. If we use Cartesian coordinates, the substrate volume element dV is dx, dy, dz . The substrate coordinate layer can be described in Fig. 9.

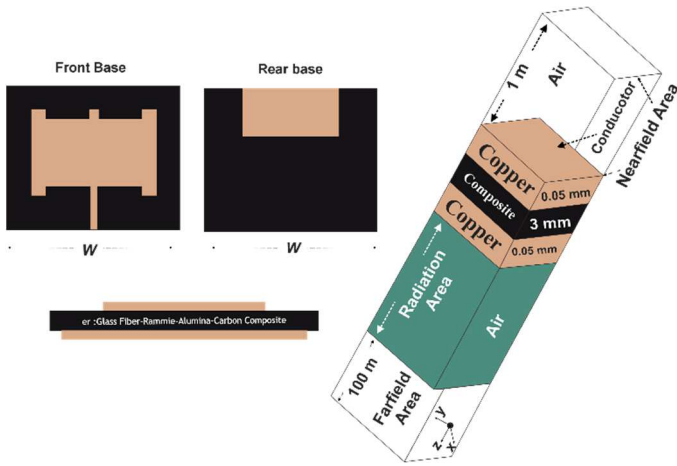


Fig. 9 Composite Layer with three Dimension coordinate analysis environment

From the capacity value, which is $C = 2.05730838 \times 10^{-10} F$, the dielectric constant can be obtained by decomposing the characteristic value of the material, which is A area of the substrate plate [29], the thickness of the material is d and ϵ_0 is the permittivity of a vacuum then with equation 3 the dielectric constant value of the substrate is $9.419967674 \approx 9.4$. This is calculated using equation 4 and 5. The dielectric constant will underline an antenna design to determine its dimensions comprehensively. Assuming that (A) and (d) are constant, and

then integrating them against the relative permittivity ϵ_r that changes along the substrate medium, it can be decomposed into equation 4.

$$C(\epsilon_r) = \int \frac{(\epsilon_0 \times A)}{d} d\epsilon_r \quad (4)$$

With equation 4, the value of capacitance C as a function of relative permittivity ϵ_r can be fulfilled. Then to implement it into a three-dimensional substrate, it is necessary to describe how the phenomenon ϵ_r , A , and d changes in the space coordinate system. Under the condition that the value of ϵ_r changes as a function of position x , y , z , it can be described by equation 5:

$$C = \iiint \frac{\epsilon_r \times \epsilon_r(x,y,z) \times A(x,y,z)}{d(x,y,z)} dV \quad (5)$$

where V is the calculated antenna substrate volume, and dV is the infinitesimal substrate volume element.

B. Asymmetrical 4x2 array

In the final stage, the 4x1 antenna array design is copied and translated down as far as the length of the ground and then put together to form a 4x2 antenna array design [30], [31]. Add a parallel connection to connect the two with a length as shown in Figure 10 as a result of the Manufacturing implementation.

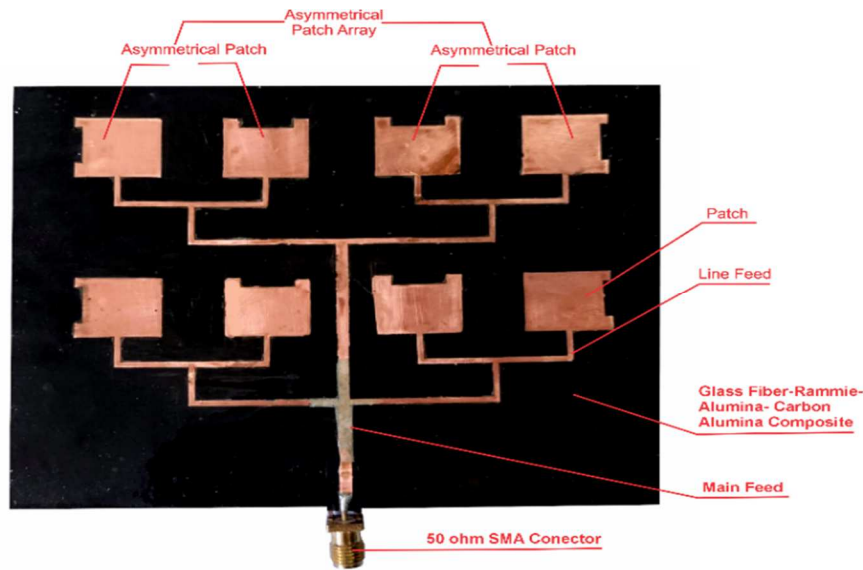


Fig. 10 4x2 Array Microstrip Antenna Manufacturing implementation

The given statement describes the final stage of designing a 4x2 antenna array. The design is created by copying and translating the 4x1 antenna array design down to the length of the ground and then connecting the two arrays in parallel. The resulting design is shown in Figure 9 [32], [33], and the specifications of the microstrip antenna array 4x2 design. The search results provide several research papers and articles related to the design of microstrip antenna arrays. These papers discuss the design and development of 4x2 microstrip patch antenna arrays for various applications, such as communication systems. The papers also discuss the optimization of the antenna arrays for increased directivity and circular polarization. Overall, the final stage of designing a 4x2 antenna array involves copying and translating the 4x1

antenna array design and connecting the two arrays in parallel. The resulting design is optimized for increased power gain and radiation pattern.

C. The Result of Antenna Array 4x2

The 4x2 array antenna test result of the return loss parameter for the proposed design and implementation of 3.5 GHz for 5G antenna using a glass fiber-Rammie-alumina composite substrate is shown in Figure 10. The targeted parameter loss achieved for the proposed antenna was less than -10 dB. The antenna 4x2 array works on the frequency 3.5841 GHz and has a value return loss of -39.49 dB.

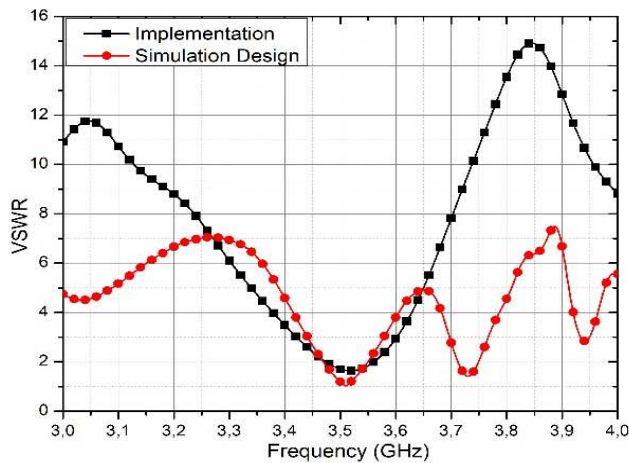


Fig. 11 The result of the VSWR Test

The tested result of the VSWR parameter is presented in Fig. 11. The targeted parameter of VSWR is less than 2, meanwhile, the tested result gets the value of 1.204584 in the frequency 3.5841 GHz, as shown in Fig. 12.

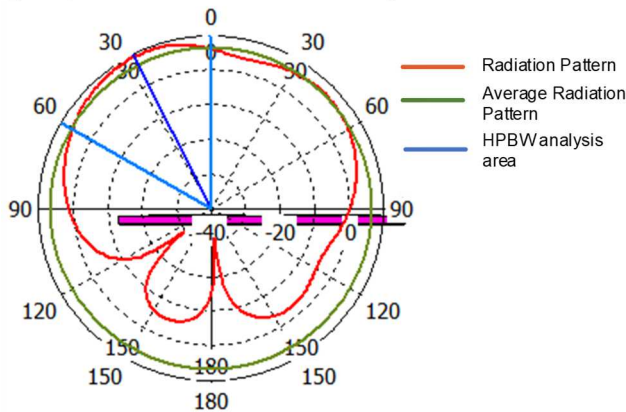


Fig.12 The tested result of the Radiation Pattern 4x2 Array Antenna

The tested result of the radiation pattern is presented in Fig. 12. The result of the radiation pattern has a main lobe magnitude of 10.9 dBi in frequency 3.5 GHz. From the tests that have been conducted in this study, it can be concluded that the 4x2 array antenna at a frequency of 3.5 GHz is used in 5G communication networks, using a glass fiber-Ramic-alumina composite substrate. Overall, the test results showed that the 4x2 array antenna with composite substrate successfully achieves the desired parameters, exhibiting good performance at the frequencies specified for use in 5G communication networks.

IV. CONCLUSION

In this work, the design of an Asymmetrical 4x2 array antenna for 5G centimeter-wave communication systems is presented. The proposed 5G configuration consists of a multi-element-antenna array combination. Each antenna array consists of four elements, which are arranged evenly, but the shape is not symmetrical between the two sides, while the two arrays are then assembled in the same arrangement with different impedance branching. Optimization of the substrate is also conducted by achieving a more efficient substrate compared to common materials. Optimization of the substrate was conducted by constructing the structure of the Glass

Fiber-Ramic-Alumina Composite compound, which has a value of $\epsilon_r = 9.4$. The proposed 5G antenna array covers the 3.5 GHz frequency band, which is dedicated to 5G cm-wave communication applications. The proposed antenna elements produce a gain of 5.23 dBi, which increased to 10.9 dBi by adopting an eight-element array configuration. By optimizing the antenna design and material substrate, antennas have the advantage of antenna characteristics applied to 5G communications in the form of characters that mutually improve electrical, mechanical, and chemical properties so that they have an extremely high molecular density that makes small leakage. Low losses, easy fabrication, and low manufacturing costs. So, the proposed structure can be a potential candidate for antennas in a more efficient mass 5G communication system. Further research can explore other composite materials by measuring the capacitance value to obtain the value of the relative dielectric constant of the composite material, because the value of the relative dielectric constant is the key so that the antenna can operate at other frequencies.

ACKNOWLEDGMENT

We express our deepest gratitude to the Indonesian National Research and Innovation Agency for the funding provided in this research. The funding was provided in collaboration with the Education Fund Management Agency of the Ministry of Finance under the Research and Innovation for Advance Indonesia funding scheme.

REFERENCES

- [1] L. Banda, M. Mzyece, and F. Mekuria, "5G Business Models for Mobile Network Operators - A Survey," *IEEE Access*, vol. 10, 2022, doi: 10.1109/access.2022.3205011.
- [2] N. O. Parchin, J. Zhang, R. A. Abd-Alhameed, G. F. Pedersen, and S. Zhang, "A planar dual-polarized phased array with broad bandwidth and quasi-endfire radiation for 5g mobile handsets," *IEEE Trans Antennas Propag.*, vol. 69, no. 10, 2021, doi:10.1109/tap.2021.3069501.
- [3] I. Mujahidin, D. A. Prasetya, Nachrowie, S. A. Sena, and P. S. Arinda, "Performance tuning of spade card antenna using mean average loss of backpropagation neural network," *International Journal of Advanced Computer Science and Applications*, 2020, doi:10.14569/ijacsa.2020.0110280.
- [4] K. Ramahatla, M. Mosalaosi, A. Yahya, and B. Basutli, "Multiband Reconfigurable Antennas for 5G Wireless and CubeSat Applications: A Review," *IEEE Access*, vol. 10, 2022, doi:10.1109/access.2022.3166223.
- [5] S. B. Damsgaard, N. J. Hernandez Marcano, M. Norremark, R. H. Jacobsen, I. Rodriguez, and P. Mogensen, "Wireless Communications for Internet of Farming: An Early 5G Measurement Study," *IEEE Access*, vol. 10, 2022, doi: 10.1109/access.2022.3211096.
- [6] E. Sonalitha *et al.*, "Combined text mining: Fuzzy clustering for opinion mining on the traditional culture arts work," *International Journal of Advanced Computer Science and Applications*, 2020, doi:10.14569/ijacsa.2020.0110838.
- [7] J. Khan, S. Ullah, U. Ali, F. A. Tahir, I. Peter, and L. Matekovits, "Design of a Millimeter-Wave MIMO Antenna Array for 5G Communication Terminals," *Sensors*, vol. 22, no. 7, 2022, doi:10.3390/s22072768.
- [8] D. A. Prasetya and I. Mujahidin, "2.4 GHz Double Loop Antenna with Hybrid Branch-Line 90-Degree Coupler for Widespread Wireless Sensor," 2020. doi: 10.1109/ecccis49483.2020.9263477.
- [9] Y. G. Adhiyoga, S. F. Rahman, C. Apriono, and E. T. Rahardjo, "Miniaturized 5G Antenna With Enhanced Gain by Using Stacked Structure of Split-Ring Resonator Array and Magneto-Dielectric Composite Material," *IEEE Access*, vol. 10, 2022, doi:10.1109/access.2022.3163285.

- [10] I. Mujahidin and A. Kitagawa, "The Novel CPW 2.4 GHz Antenna with Parallel Hybrid Electromagnetic Solar for IoT Energy Harvesting and Wireless Sensors," *International Journal of Advanced Computer Science and Applications*, vol. 12, no. 8, 2021, doi:10.14569/ijacsa.2021.0120845.
- [11] S. Dey, M. S. Arefin, and N. C. Karmakar, "Design and Experimental Analysis of a Novel Compact and Flexible Super Wide Band Antenna for 5G," *IEEE Access*, vol. 9, 2021, doi:10.1109/access.2021.3068082.
- [12] I. Mujahidin and A. Kitagawa, "The Compact 2.4 GHz Hybrid Electromagnetic Solar Energy Harvesting (HES-EH) circuit using Seven Stage Voltage Doubler and Organic Thin Film Solar Cell," in *2021 4th International Seminar on Research of Information Technology and Intelligent Systems, ISRITI 2021*, 2021, doi:10.1109/isriti54043.2021.9702844.
- [13] N. M. El-Wazery, M. I. El-Elamy, and S. H. Zoalfakar, "Mechanical properties of glass fiber reinforced polyester composites," *Int. J. Appl. Sci. Eng.*, vol. 14, pp. 121-131, 2017.
- [14] P. Sadeghi, Q. Cao, R. Abouzeid, M. Shayan, M. Koo, and Q. Wu, "Experimental and Statistical Investigations for Tensile Properties of Hemp Fibers," *Fibers*, vol. 12, no. 11, p. 94, Nov. 2024, doi:10.3390/fib12110094.
- [15] O. R. Alobaidi *et al.*, "Vacuum annealed Ga:ZnO (GZO) thin films for solar cell integrated transparent antenna application," *Mater Lett*, vol. 304, 2021, doi: 10.1016/j.matlet.2021.130551.
- [16] S. Sarjoghian, Y. Alfadhli, X. Chen, and C. G. Parini, "A 3-D-Printed High-Dielectric Materials-Filled Pyramidal Double-Ridged Horn Antenna for Abdominal Fat Measurement System," *IEEE Trans Antennas Propag*, vol. 69, no. 1, 2021, doi:10.1109/tap.2020.3008653.
- [17] H. A. Elmobarak, M. Himdi, X. Castel, S. K. A. Rahim, and T. K. Geok, "Flexible Patch Antenna Array Operating at Microwaves Based on Thin Composite Material," *IEEE Access*, vol. 10, 2022, doi:10.1109/access.2022.3218342.
- [18] S. Ma, X. N. Li, Z. D. Li, and J. J. Ding, "Electronic Beam Steering Metamaterial Antenna with Dual-Tuned Mode of Liquid Crystal Material," *Sensors*, vol. 23, no. 5, 2023, doi: 10.3390/s23052556.
- [19] H. Van Damme, "Concrete material science: Past, present, and future innovations," *Cement and Concrete Research*. 2018. doi:10.1016/j.cemconres.2018.05.002.
- [20] Y. Fu, T. Shen, J. Dou, and Z. Chen, "Absorbing Material of Button Antenna with Directional Radiation of High Gain for P2V Communication," *Sensors*, vol. 23, no. 11, 2023, doi:10.3390/s23115195.
- [21] Y. I. Abdulkarim *et al.*, "Design of a broadband coplanar waveguide-fed antenna incorporating organic solar cells with 100% insolation for ku band satellite communication," *Materials*, vol. 13, no. 1, 2020, doi:10.3390/ma13010142.
- [22] X. Yi, C. Cho, J. Cooper, Y. Wang, M. M. Tentzeris, and R. T. Leon, "Passive wireless antenna sensor for strain and crack sensing - Electromagnetic modeling, simulation, and testing," *Smart Mater Struct*, 2013, doi: 10.1088/0964-1726/22/8/085009.
- [23] Q. Xia *et al.*, "High temperature microwave absorbing materials," *J Mater Chem C Mater*, 2023, doi: 10.1039/d2tc04671g.
- [24] M. N. Abbasi, A. Aziz, K. A. Aljaloud, A. R. Chishti, Y. T. Aladadi, and R. Hussain, "A Close Proximity 2-Element MIMO Antenna Using Optically Transparent Wired-Metal Mesh and Polyethylene Terephthalate Material," *IEEE Access*, vol. 11, 2023, doi:10.1109/access.2023.3298568.
- [25] A. Tamang *et al.*, "Combining Photosynthesis and Photovoltaics: A Hybrid Energy-Harvesting System Using Optical Antennas," *ACS Appl Mater Interfaces*, vol. 12, no. 36, 2020, doi:10.1021/acsami.0c09007.
- [26] H. C. Huang and J. Lu, "Evolution of Innovative 5G Millimeter-Wave Antenna Designs Integrating Non-Millimeter-Wave Antenna Functions Based on Antenna-in-Package (AiP) Solution to Cellular Phones," *IEEE Access*, vol. 9, 2021, doi:10.1109/access.2021.3077309.
- [27] W. Hong, K. H. Baek, and S. Ko, "Millimeter-Wave 5G Antennas for Smartphones: Overview and Experimental Demonstration," *IEEE Trans Antennas Propag*, 2017, doi: 10.1109/tap.2017.2740963.
- [28] K. A. Fante and M. T. Gameda, "Broadband microstrip patch antenna at 28 GHz for 5G wireless applications," *International Journal of Electrical and Computer Engineering*, vol. 11, no. 3, 2021, doi:10.11591/ijece.v11i3.pp2238-2244.
- [29] J. Zhang, X. Ge, Q. Li, M. Guizani, and Y. Zhang, "5G Millimeter-Wave Antenna Array: Design and Challenges," *IEEE Wirel Commun*, 2017, doi: 10.1109/MWC.2016.1400374RP.
- [30] H. Kim and S. Nam, "Performance Enhancement of 5G Millimeter Wave Antenna Module Integrated Tablet Device," *IEEE Trans Antennas Propag*, vol. 69, no. 7, 2021, doi:10.1109/tap.2020.3044651.
- [31] A. Suharjo *et al.*, "Performance Evaluation of LoRa 915 MHz for IoT Communication System on Indonesian Railway Tracks with Environmental Factor Propagation Analysis," in *Proceedings of the 2023 IEEE International Conference on Industry 4.0, Artificial Intelligence, and Communications Technology, IAICT 2023*, 2023. doi: 10.1109/iaict59002.2023.10205909.
- [32] S. Tariq, S. I. Naqvi, N. Hussain, and Y. Amin, "A Metasurface-Based MIMO Antenna for 5G Millimeter-Wave Applications," *IEEE Access*, vol. 9, 2021, doi: 10.1109/access.2021.3069185.
- [33] I. Mujahidin and A. Kitagawa, "Ring slot CP antenna for the hybrid electromagnetic solar energy harvesting and IoT application," *Telkonnika (Telecommunication Computing Electronics and Control)*, vol. 21, no. 2, pp. 290-301, Apr. 2023, doi:10.12928/telkonnika.v21i2.24739.